Recursive numerical solution for nonlinear wave propagation in fibers and cylindrically symmetric systems

Sami T. Hendow and Sami A. Shakir

An efficient and compact recursive numerical solution of the wave equation is developed and applied to cylindrically symmetric optical systems. Numerical results are given for wave propagation through an aperture and in linear and nonlinear optical fibers. This code is most useful for multiwave mixing and wave propagation in nonlinear media.

I. Introduction

The evolution of a propagating wave front is fully described by the solution of the wave equation. There are two basic types of numerical solution. The first is based on the well-known diffraction integral of Rayleigh and Sommerfeld,[1,2] and the second is the direct numerical solution of the second-order differential wave equation.

In most practical cases the integral formula of Rayleigh and Sommerfeld results in an excellent solution for the propagated field. Some of the techniques that may be employed to simplify the calculations are the specialization of the integral to the Fresnel or Fraunhofer zones and the use of the properties of fast Fourier transforms and shift invariant systems.[3] However, Fresnel and Fraunhofer formulas have certain limitations. They are not suitable for cases where the medium of propagation is locally varying, such as when the index is a nonlinear function of the field intensity. Propagation codes based on this solution tend to be slow for propagation zones prior to the Fresnel zone, i.e., close to the initial starting plane. These solutions in general do not provide an easy handle for treating the coupling of propagating waves, such as in multiwave mixing.

The second category employed for the propagation of a wave is the direct numerical solution of the wave equation. In this case the partial derivatives in the wave equation are replaced by their numerical equivalent, and the field is propagated one step in time by solving a coupled set of equations.[4,5] Currently, a popular method for wave propagation is the beam propagation method,[6–8] which utilizes the finite Fourier series representation to propagate the wave equation an incremental step. Such solutions have the advantages that the medium's polarization (i.e., complex index of refraction) is allowed to be locally varying and that coupling between propagating fields is relatively easy to handle. In addition, all the intermediate variations of the wave along the propagation direction are also obtained. The disadvantages of this method is in its structured solution. The field is written in terms of a coupled set of equations that are solved numerically. Such solutions often require tedious matrix inversions which require a mainframe computer for fast number crunching.

This paper presents an alternative technique based on the direct numerical solution of the wave equation. The difficulties discussed above are bypassed by employing recursive mathematical solutions[9] that speed up the calculation appreciably without giving up the advantages of the direct solution of the wave equation. The formalism presented here is general and does not depend on details of the wave equation.

II. General Integration Technique

Our main interest is solving the wave equation in the paraxial approximation as represented by the following operator equation:

$$\hat{H}(r,\phi,E)E = i\frac{\partial E}{\partial z}, \tag{1}$$

where the axis of propagation is the z axis, and r is the transverse coordinate. The electric field $E(r,\phi,z)$ is the time-independent factor of the general electric field as defined by

Sami T. Hendow is with Litton Guidance and Control Systems, 5500 Canoga Avenue, Woodland Hills, California 91367; S. A. Shakir is with University of New Mexico, Institute for Modern Optics, Albuquerque, New Mexico 87131.

Received 15 February 1986.
0003-6935/86/111759-06$02.00/0.

$$\mathcal{E}(r,\phi,z,t) = E(r,\phi,z)\exp[i(k_z z - wt)]. \quad (2)$$

The operator $\hat{H}$ in Eq. (1) represents transverse derivatives and any other factors such as nonlinear terms and angular ϕ dependent terms, as exemplified by the wave equation (in cylindrical coordinates)

$$\left\{\frac{\partial^2}{\partial r^2} + \frac{1}{r}\frac{\partial}{\partial r} + \frac{1}{r^2}\frac{\partial^2}{\partial \phi^2} + [k_0^2 n^2 - k_z^2 + f(E)]\right\}E = -2ik_z\frac{\partial E}{\partial z}, \quad (3)$$

where k_z is the axial component of the k vector nk, n is the complex index of refraction of the medium, and $z/2k_z = \tilde{z}$. Any linear transverse variations of the index of refraction are accounted for through the term $n(r,\phi)$ as is necessary for waveguides. Nonlinearities are taken into account through the term $f(E)$. Assuming cylindrical symmetry, the 3-D problem is reduced mathematically to two dimensions, i.e., one transverse coordinate. The case of a nonlinear planar waveguide is another example of a 2-D model which can be used to illustrate the technique. Dropping the ϕ dependence, the formal solution of Eq. (1) is

$$E(r,\tilde{z} + \Delta z) = \exp(i\Delta z\hat{H})E(r,\tilde{z}), \quad (4)$$

where Δz is the integration interval along the z axis and is assumed to be small so that $f[E(r,z)]$ does not change much during this interval. To solve the problem numerically, the complex exponential operator is approximated by a complex rational operator,[9]

$$\exp(i\Delta z\hat{H}) \simeq \frac{\hat{1} + i^1/_2\,\Delta z\hat{H}}{\hat{1} - i^1/_2\,\Delta z\hat{H}}. \quad (5)$$

Unlike the relatively inaccurate first-order Taylor approximation of the complex exponential operator, this approximation is correct to second order and for the lossless case and is a unitary operator like the exponential operator it approximates. This is a useful property as the total energy during propagation remains stable despite the approximation (5). Substituting (5) into (4), an explicit equation results:

$$\left[\hat{1} - \frac{i\Delta z}{2}\hat{H}\right]E^{n+1} = \left[\hat{1} + \frac{i\Delta z}{2}\hat{H}\right]E^n. \quad (6)$$

The $n+1$ and n superscripts denote the $n+1$st and nth integration plane, i.e., $\tilde{z} + \Delta z$ and $\tilde{z}$, respectively. Using the three-point approximation of the first- and second-order radial derivatives of the field E, Eq. (6) can always be written and regardless of the details of the problem at hand, in the following form:

$$a_j E_{j+1}^{n+1} + b_j E_j^{n+1} + c_j E_{j-1}^{n+1} = F_j^n. \quad (7)$$

Here $r = j\Delta r$, $\tilde{z} = n\Delta z$, and Δr and Δz are the radial and axial increments, respectively. F_j is the right-hand side of Eq. (6) evaluated at the point $r = j\Delta r$ and at the plane $\tilde{z} = n\Delta z$. The coefficients a_j, b_j, and c_j are generally a function of r, and their functional dependence is usually a simple algebraic one which can be worked out by casting the particular wave equation into the form of Eq. (7). This is always possible for the three-point approximation of the derivatives. The right-hand side of Eq. (7) is the known initial profile, while the left-hand side is in terms of three unknown quantities on the radial plane at $\tilde{z} = (n+1)\Delta z$.

From Eq. (7), a radial field grid containing J elements leads to a coupled set of J equations describing the field at all points in space. These equations may be solved for the field using conventional methods which require handling a J × J matrix. This, however, leads to a cumbersome propagation code. This problem is avoided by reducing Eq. (7) to a recursive relation relating the values at two points on the plane $(n+1)$. Assuming that one of the electric field terms can be written in terms of one of the other two terms, the following relation is postulated:

$$E_j^{n+1} = \alpha_{j+1}^n E_{j+1}^{n+1} + \beta_{j+1}^n, \quad (8)$$

where α_j^n and β_j^n are auxiliary functions that are found by using Eq. (8) for the $j-1$ term in Eq. (7). After collecting terms we get

$$E_j^{n+1} = \left(-\frac{a_j}{b_j + c_j\alpha_j^n}\right)E_{j+1}^{n+1} + \frac{F_j^n - c_j\beta_j}{b_j + c_j\alpha_j^n}. \quad (9)$$

Comparing Eqs. (8) and (9) and equating the corresponding coefficients in both equations, the following recursion relations for α_j^n and β_j^n are derived;

$$\alpha_j^n = -\frac{b_j}{c_j} - \frac{a_j}{c_j\alpha_{j+1}^n}; \quad (10a)$$

$$\beta_j^n = \frac{F_j^n}{c_j} + \frac{a_j}{c_j}\frac{\beta_{j+1}^n}{\alpha_{j+1}^n}. \quad (10b)$$

To start the recursive computation, initial values in Eqs. (8) and (10) are needed. At this point the boundary values of the problem are introduced. In Cartesian coordinates, the usual boundary conditions are to set the field to zero at the extreme tranverse points along the x axis. For cylindrical coordinates it is more natural to take the origin ($r = 0$) and the outer boundary ($r = R_{\max}$) as the fixed boundary points. To do so, it is necessary to transform the physical field into a scaled field

$$\tilde{E}(r,\tilde{z}) = rE(r,\tilde{z}). \quad (11)$$

This insures that $\tilde{E}(r = 0,\tilde{z}) = 0$ for all $\tilde{z}$. Of course, one cant take the two extreme radial points $r = \pm R_{\max}$ as the boundary points, but then half of the calculated points are redundant due to the radial symmetry of the problem. Hence adopting the definition in Eq. (11) reduces the computational time by half. In this case,

$$\tilde{E}_0^n = \tilde{E}_J^n = 0, \quad (12)$$

where $R_{\max} = J\Delta r$. Moreover, applying Eq. (7) to the case $j = J$ and employing Eq. (12), one obtains

$$\tilde{E}_{J-2}^{n+1} = -\frac{b_{J-1}}{c_{J-1}}\tilde{E}_{J-1}^{n+1} + \frac{F_{J-1}^n}{c_{J-1}}. \quad (13)$$

The starting values for Eq. (10) are obtained by comparing Eqs. (13) to (8) with $j = J-2$ and also by using Eqs. (12) in (8) for $j = 0$. These values are

$$\alpha_{J-1}^n = -\frac{b_{J-1}}{c_{J-1}}, \quad \beta_{J-1}^n = \frac{F_{J-1}^n}{c_{J-1}}, \quad \tilde{E}_i^n = -\frac{\beta_1^n}{\alpha_1^n}. \tag{14}$$

Finally, using Eq. (14) in (10), the auxiliary functions are computed for all j. The field on the plane $(n+1)$ is calculated by using the recursion relation of Eq. (8).

To summarize: given a linear or nonlinear wave equation, it is converted into a difference equation similar to Eq. (7) by employing the solution in Eq. (6). Knowing the field at the nth plane, one can propagate it to the next plane $(n+1)$ by employing the following steps.

First compute the auxiliary functions in Eqs. (10) starting with Eq. (14). Once α_j^n and β_j^n are computed for all $0 < j < J$, the field is computed using Eq. (8) and starting with $E_0^{n+1} = 0$. Note that one boundary condition is used for the solution of Eq. (10), while the other is used for the solution of Eq. (8). For the case where cylindrical coordinates are adopted, the transformation (11) is useful.

To illustrate the procedure, it is applied to the nonlinear wave equation depicted in Eq. (3). Replacing E by $\tilde{E}/r$, the scaled wave equation becomes

$$\hat{H}\tilde{E} = \left\{\frac{\partial^2}{\partial r^2} - \frac{1}{r}\frac{\partial}{\partial r} + \left[k_0^2 n^2(r) - k_z^2 + \frac{1}{r^2} + \frac{f(\tilde{E})}{r}\right]\right\}\tilde{E}(r,\tilde{z}) = i\frac{\partial \tilde{E}}{\partial \tilde{z}}. \tag{15}$$

Using the three-point expansion, $\partial\tilde{E}_j/\partial r = (\tilde{E}_{j+1} - \tilde{E}_{j-1})/2\Delta r + O(\Delta r^3)$, $\partial^2\tilde{E}_j/\partial r^2 = (\tilde{E}_{j+1} - 2\tilde{E}_j + \tilde{E}_{j-1})/\Delta r^2 + O(\Delta r^3)$ in Eq. (15), a difference equation similar to Eq. (7) is obtained with

$$a_j = 1 - \frac{1}{2j}, \qquad c_j = 1 + \frac{1}{2j},$$

$$b_j = \Delta r^2[k_0^2 n^2(r) - k_z^2 + f(\tilde{E}/r)] + \frac{1}{j^2} - 2 + i\gamma, \tag{16}$$

$$F_j^n = -a_j\tilde{E}_{j+1}^n - (b_j - 2i\gamma)\tilde{E}_j^n - c_j\tilde{E}_{j-1}^n,$$

where $\gamma = 2\Delta r^2/\Delta z$. It is useful to note that for linear problems the coefficients a_j, b_j, and c_j are independent of $\tilde{z}$, which implies that the auxiliary function α_j^n is independent of $\tilde{z}$ and hence can be computed only once and used for all $\tilde{z}$. This saves computer time.

An important point to consider is the appropriate radial (Δr) and axial (Δz) mesh sizes. From the sampling theorem, the minimum sampling rate for the radial field distribution should be at least twice the highest frequency component present in that distribution. For example,[1] a rectangular profile of width $2x_w$ has a spectrum of $2x_w\,\mathrm{sinc}(2x_w f)$, where f is the spatial frequency. If we take the highest frequency component to be $f_{\max} = 10/2x_w$, the radial increment should be less than one-tenth of the smallest width the beam acquires during propagation. This is an important consideration for tightly focused beams. To estimate the step size Δz, an inspection of Eq. (7) suggests that

$$\Delta z \ll \frac{8\pi\epsilon^2}{\lambda}. \tag{17}$$

III. Extensions

The method discussed above is of second order in z and r. It can be shown that the accuracy along the propagation axis can be improved to third order in Δz by employing a two-step technique. The field is first propagated in two steps $\Delta z/2$ each. Then the computation is repeated with a single step Δz. Assuming that the field distribution calculated by the two step run is $\tilde{E}_{j1}^{n+1}$ and the result for the single-step computation $\tilde{E}_{j2}^{n+1}$, a better result is obtained by a weighted average of the two as

$$\tilde{E}_j^{n+1} = \frac{4\tilde{E}_{j1}^{n+1} - \tilde{E}_{j2}^{n+1}}{3} + O(\Delta z^4). \tag{18}$$

The recursive technique employed here can easily be extended to 3-D problems. Again cylindrical coordinates are assumed, and the 3-D function is represented by a complete set of circular harmonics. As shown in the Appendix, the problem reduces to a set of coupled equations whereby each equation can be solved using the recursive technique of Sec. II. The extension of the field in terms of the cylindrical harmonics is attractive since in many cases of interest one is interested in only the first few harmonics.

Equations (1)–(3) are scalar equations. If needed, a polarization vector may be added to the field. The solution then proceeds by projecting the field and the corresponding wave equation onto the unit orthogonal polarization set of choice. This transforms the problem into the more involved solution of a coupled set of wave equations for the polarization components. These equations are decoupled only for the linear-index case.

IV. Numerical Results

A computer code is developed and applied to a variety of problems ranging from reflection off a nonlinear interface[4] and high-gain Raman scattering[10] to propagation inside nonlinear fibers. The numerical results are also checked against experimental[11] and analytical[1] results. Some of these are given in Figs. 1–4.

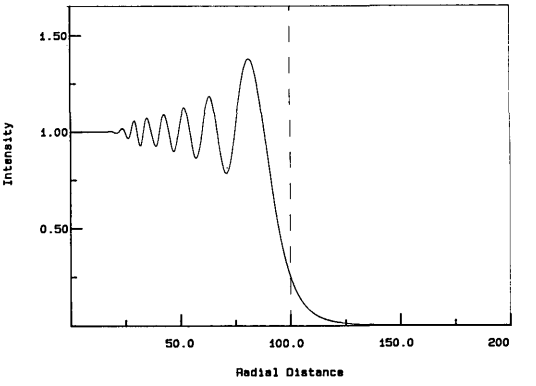

Fig. 1. Diffraction of a plane wave through a circular aperture of 200λ diameter. The propagation distance is 500λ, and the medium's index is 1. The radial increment is 0.33λ, while the integration interval is 10λ. λ is the field wavelength. The dashed line represents the edge of the aperture.

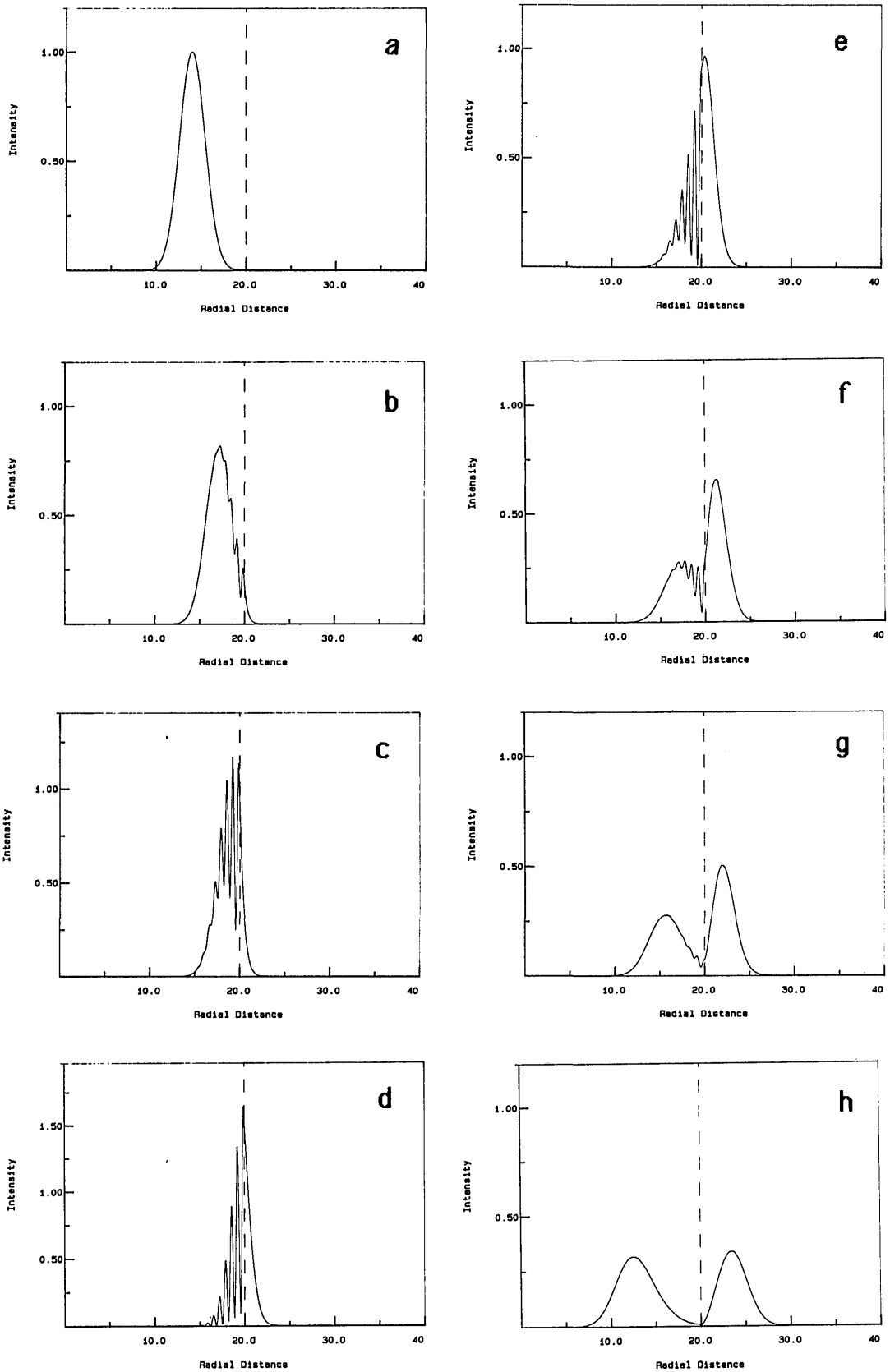

Fig. 2. Reflection and refraction of a Gaussian doughnut wave packet in an optical fiber. The core index is 1.5, and the cladding index is 1.32. The wave angle of incidence with the normal to the cladding is 60°. The fiber diameter is 40λ; axial and radial increments are 0.8λ and 0.067λ, respectively. The frames are for propagation distances of (a) $z = 0$, (b) $z = 6.4\lambda$, (c) $z = 9.6\lambda$, (d) $z = 12.8\lambda$, (e) $z = 16\lambda$, (f) $z = 19.2\lambda$, (g) $z = 22.4\lambda$, (h) $z = 28.8\lambda$. The dashed line represents the boundary between the core and cladding. The horizontal axis is in units of λ.

Figure 1 shows the propagation of a top-hat wave of wavelength λ. The dashed line represents the edge of the aperture, and Fresnel diffraction is clearly evident. An exponential field attenuator with an $1/e$ halfwidth of 2.67λ is used to smooth the sharp truncation effect of the aperture edge. This removes a ripple noise effect that shows up in the propagated field which is attributed to the limited accuracy of the three-point approximation of the derivatives. Of course, a five-point expansion of the derivatives is more accurate. However, the recursive formula in Eq. (8) is not suitable for this higher-order expansion of the derivatives. The calculation is also repeated without the use of Eq. (11) and with the boundaries at $r = \pm J\Delta r$. The results were identical in both cases. Equation (15) is not well defined for $r = 0$. Hence the origin is bypassed by shifting the array points half a point, i.e., $r_j = (j + 1/2)\Delta r$.

Figure 2 shows a Gaussian annular wave propagating in a cylinder of index 1.5 and diameter = 20λ. The cladding index is 1.32. The wave is chosen to approach the wall of the cylinder at an angle of incidence of 60° with reflection and refraction shown in successive frames. The physical wave, therefore, looks like expanding and contracting annular waves. Changing the cladding index to 1.0 leads to total internal reflection.

The two cases above use a linear index for the medium. Figure 3 shows a Gaussian wave propagating in a nonlinear medium. An exaggerated nonlinearity in the index is chosen as $n(r) = 1.5 \pm I(r)$, where I is the intensity of the wave. As expected, self-focusing and defocusing of the wave with propagation are clear.

The case of nonlinear cladding is shown in Fig. 4. As in Fig. 2, the initial field distribution is annular and Gaussian in shape. In contrast to slab nonlinear waveguides, this structure has a doughnut cross section. The cladding index n_c is chosen as $n_c = 1.0 + I(r)$. As expected, this figure shows the penetration of the field into the cladding and the generation and localization of a nonlinear propagating wave near the core–cladding interface. The field in this case is trapped in a self-focused thin film of high index, which is driven by the high nonlinearity of the cladding and high intensity of the penetrated field. This region of high index also acts as a boundary preventing further penetration of the field.

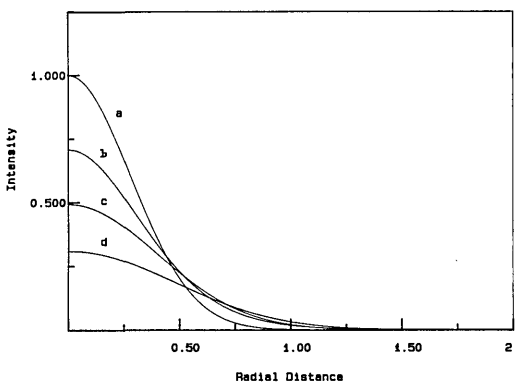

Fig. 3. Axial propagation of a Gaussian wave in a nonlinear medium. The axial and radial increments are 20λ and 0.08λ, respectively. The intial wave at $z = 0$ is (a), while (b)–(d) are the propagated waves at $z = 600\lambda$. The nonlinear index of the medium is (b) $n = 1.5 + I(r)$, (c) $n = 1.5$, (d) $n = 1.5\text{-}I(r)$, where I is the intensity of the wave at the radial distance r. The point $r = 1$ corresponds to 20λ.

The field maximum is adjacent to the interface and also varies with propagation distance depending on the field in the neighboring areas. Reducing the nonlinearity to $n_c = 1.0 + 0.5I$ leads to reflection of the incident wave without formation of a trapping region.[4] Similar behavior also exists in thin film slabs with a nonlinear cladding, where the field maximum is drawn out of the film and a self-focused planar channel results at high powers in the cladding.[12]

In conclusion, a recursive numerical approach to the solution of wave propagation has been presented. The method is relatively simple to program and leads to a stable efficient code. This method is most useful for quided waves and high-gain multiwave interactions where the Fresnel diffraction integral is not adequate.

Stability, modest memory requirements, and efficiency make this approach well suited for personal desktop computers. Actually, all the examples in this paper were done on an IBM XT microcomputer. The calculations were performed in FORTRAN with an execution time of ~2s/propagation step (Δz) for the linear-index case and for a 250-point radial array.

Preliminary results were presented at the Optical Society of American Annual meeting, Oct. 1985 [see J. Opt. Soc. Am. A 2 (13), p 36 (1985)].

Appendix: Extension to Three Dimensions

The radially nonsymmetric case (e.g., nonsymmetric input field or index of the medium) may be treated by decomposing the field and the wave equation in terms of the normal modes of the guide. The normal modes are found by solving the steady-state case where $\partial E/\partial z = 0$. Using the separation of variables, $E(r,\phi) = R(r)\Phi(\phi)$, the wave equation separates to a radial and angular part. The solution of the angular part is $\Phi(\phi) = \cos\phi l$, where l is an integer. Let us then expand $E(r,\phi,z)$ in terms of the complete set $[\cos\phi l]$,

$$E(r,\phi,\tilde{z}) = \sum_{l=0}^{\infty} R_l(r,\tilde{z})\cos\phi l. \tag{A1}$$

Substituting Eq. (18) in Eq. (3) and projecting onto the mth mode, we get the following coupled set of wave equations:

$$\frac{\partial^2 R_m}{\partial r^2} + \frac{1}{r}\frac{\partial R_m}{\partial r} + \left[n^2 k_0^2 - k_z^2 - \frac{m^2}{r^2} + \langle V_{NL}\rangle\right] R_m = i2k_z \frac{\partial R_m}{\partial z}, \tag{A2}$$

$$\langle V_{NL}\rangle = \frac{1}{\pi}\int_0^{2\pi} k_0^2 n_{NL}^2(r,\phi)\cos l\phi\cos m\phi, \tag{A3}$$

where n_{NL} is the nonlinear part of the index. These equations are decoupled for the linear-index case and

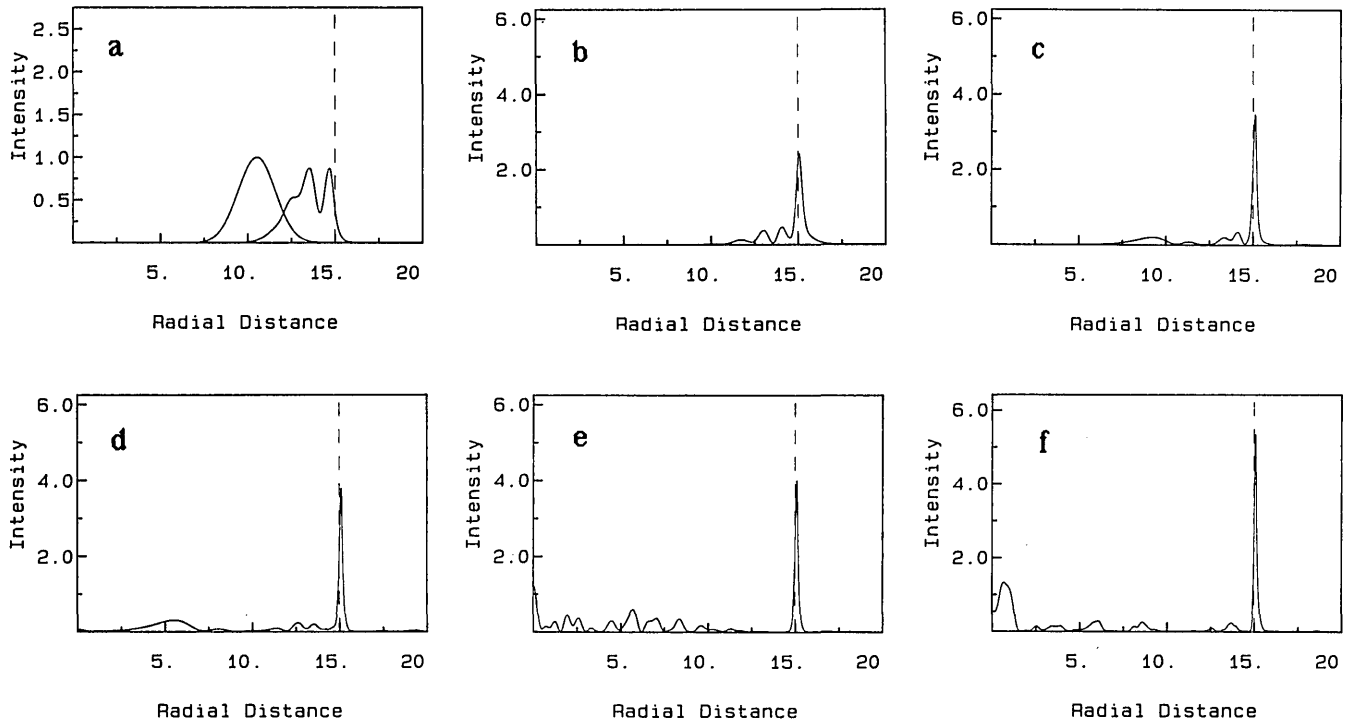

Fig. 4. Reflection of a Gaussian doughnut wave by a nonlinear interface. The cladding index is $1.0 + I(r)$, and the fiber's diameter is 15λ. The axial and radial increments are 0.5λ and 0.01667λ, respectively. Other parameters are as in Fig. 2. Propagation distances are (a) 0 and 3λ, (b) 6λ, (c) 9λ, (d) 12λ, (e) 21λ, (f) 102λ. The radial distance of 20 corresponds to 10λ.

are coupled when the index is nonlinear. The solution is obtained by solving the coupled set of wave equations for the individual components and for each propagating step.

References

1. J. W. Goodman, *Introduction to Fourier Optics* (McGraw-Hill, New York, 1968).
2. A. G. Fox and T. Li, "Resonant Modes in a Maser Interferometer," Bell Syst. Tech. J. **40**, 453 (1961).
3. G. N. Lawrence and P. N. Wolfe, "Applications of the LOTS Computer Code to Laser Fusion Systems and Other Physical Optics Problems," Proc. Soc. Photo-Opt. Instrum. Eng. **190**, 238 (1979).
4. W. J. Tomlinson, J. P. Gordon, P. W. Smith, and A. E. Kaplan, "Reflection of a Gaussian Beam at a Nonlinear Interface," Appl. Opt. **21**, 2041 (1982) and references therein.
5. W. J. Tomlinson, R. H. Stolen, and A. M. Johnson, "Optical Wave Breaking of Pulses in Nonlinear Optical Fibers," Opt. Lett. **10**, 457 (1985).
6. J. A. Fleck, R. R. Morris, and E. S. Bliss, "Small Scale Self-Focusing Effects in a High Power Glass Laser Amplifier," IEEE J. Quantum Electron. **QE-14**, 353 (1978) and references therein.
7. A. E. Siegman, "Quasi fast Hankel Transform," Opt. Lett. **1**, 13 (1977).
8. M. Lax *et al.*, "Electromagnetic Field Distribution in Loaded Unstable Resonators," J. Opt. Soc. Am. A **2**, 731 (1985).
9. A. Goldberg, H. M. Schey, and J. L. Schwarz, "Computer-Generated Motion Pictures of One-Dimensional Quantum-Mechanical Transmission and Reflection Phenomena," Am. J. Phys. **35**, 177 (1967).
10. K. Druhl, S. A. Shakir, and M. Yusuf, "Stokes Beam Parameters at Large Gain for Focused Pump Beams," Opt. Lett. (July 1986).
11. Y. Li and H. Platzer, "An Experimental Investigation of Diffraction Patterns on Low-Fresnel-Number Focusing Systems," Opt. Acta **30**, 1621 (1983).
12. C. T. Seaton, J. E. Valera, R. L. Shoemaker, G. I. Stegeman, J. T. Chilwell, and S. D. Smith, "Calculation of Nonlinear TE Waves Guided by Thin Dielectric Films Bounded by Nonlinear Media," IEEE J. Quantum Electron. **QE-21**, 774 (1985).